

Inhibition effect of Tantum Rosa drug on the corrosion of copper in 3.5 wt.% NaCl solution

Simona Varvara*, Gianina Damian, Roxana Bostan, Maria Popa

Department of Cadastre, Civil Engineering and Environmental Engineering, "1 Decembrie 1918", University of Alba Iulia, 15-17 Unirii St., Alba-Iulia 510009, Romania

*E-mail: svarvara@uab.ro

Received: 1 May 2022 / Accepted: 29 June 2022 / Published: 7 August 2022

In the present paper, the inhibition performance of benzydamine hydrochloride drug, commercially named Tantum Rosa on copper was investigated in 3.5 wt.% NaCl solution. Potentiodynamic polarization, electrochemical impedance spectroscopy, scanning electron microscopy and energy dispersive X-ray spectroscopy were employed. The electrochemical results revealed that Tantum Rosa acts as a mixed-type inhibitor on the copper corrosion and its protective effectiveness is concentration and time-dependent. The inhibiting efficiency of Tantum Rosa was improved with the increase in the drug concentration and reached the maximum value of 91.5% at 5 mM. The inhibitive effect of Tantum Rosa was afforded to its spontaneous adsorption on the copper surface, through combined physical and chemical processes, according to Langmuir adsorption isotherm. The time-weakening of the inhibitor film stability led to a progressive decay of the inhibition ability of Tantum Rosa at prolonged exposure. SEM-EDX analysis confirmed that the surface morphology of copper was significantly improved in the presence of the inhibitor.

Keywords: copper, drug, corrosion inhibitor, EIS, potentiodynamic polarization, SEM-EDX

1. INTRODUCTION

Pharmaceutical products offer multiple benefits, including curing diseases, alleviating symptoms, and improving the quality of life, but the ones that remained unused or expired might cause important environmental problems [1, 2]. Currently, a part of expired or unused drugs is destroyed by incineration, and thus toxic compounds containing nitrogen, sulfur, phosphorus, fluorine, and chlorine are released into the atmosphere. Another part is stored generating soiled waste accumulations [3]. The drugs might be also released in residual waters, since pharmaceutical contaminants have been detected globally in the surface waters [4], groundwaters [5], and drinking waters [6].

Recently, various management strategies and green pharmaceutical practices, including environmental research on medicinal products, sustainable supply and use of medication, proper waste

disposal management [1] and a greener community pharmacy were applied in the attempt to minimize the environmental impact of pharmaceutical wastes [7].

Following the circular economy concept, another way to solve the economic and environmental problems associated to the disposal and the treatment of the expired drugs could be their reutilization for other purposes [8, 9], such as the protection of the metals against corrosion.

In the last years [10-12], numerous pharmaceutical drugs have been explored and reported as efficient corrosion inhibitors for different metals and alloys in various environments. As formerly mentioned [10, 11, 13], many drugs possess heteroatoms (*i.e.*, P, N, O, and S) with lone electron pairs and/or multiple conjugated bonds with delocalized electrons in their molecules, presenting considerable similarities with the molecular structures of the conventional organic corrosion inhibitors. These features facilitate the adsorption of the drug molecules on the metals surface and the formation of protective barrier films, which are able to suppress the corrosion process.

Several literature reviews [3, 12, 14- 24] summarize the inhibiting efficiencies of various drugs on different metals in several corrosive electrolytes.

However, in the particular case of the copper corrosion in saline environments, the number of studies [25-32] reporting the inhibiting properties of the chemical medicines is rather limited. For instance, domperidone drug was found to be an efficient anodic inhibitor of copper in 3.5 wt.% NaCl solution, achieving a maximum protective efficiency of 94.2% at a concentration of 20 mg L⁻¹ [27]. The theoretical calculations revealed that domperidone molecules could be adsorbed on the copper surface in a closely parallel manner through the imidazolidinone ring and benzene ring [27]. Azithromycin [25] and cephadrine [28] were also reported as effective corrosion inhibitors for copper in 0.9 wt.% NaCl solution. The adsorption of cephadrine on copper surface occurs through the β -laktam ring and side chain [28], while in the case of azithromycin, the protonated form was involved in the adsorption process. S. Zor [26] has also shown that sulfathiazole drug is able to act as a cathodic inhibitor for copper in 0.1 M NaCl solution. Nicotinamide, one of the two forms of vitamin B₃ [30] and doxepin, a tricyclic antidepressant drug [29] have been also proved as good mixed-type inhibitors of copper corrosion in 3.5 wt.% NaCl solution. The inhibition of copper corrosion by nicotinamide was achieved through its adsorption on the metal surface and the formation of a complex with Cu⁺ ions, thus preventing the further development of the chloride complexes [30]. In the case of doxepin, based on the theoretical calculation, it was assumed that the nitrogen atom from the drug molecule is mainly involved in the electron donation to the copper unoccupied orbitals, leading to the formation of an insoluble and highly adherent donor-acceptor complex on the metal surface [29].

Continuing our research work investigating the anticorrosive properties of several drugs on copper-based materials [29, 33], in the present paper we have explored the inhibiting effect of Tantum Rosa toward the corrosion of copper in 3.5 wt.% NaCl solution. Tantum rosa is a water-soluble non-steroidal anti-inflammatory medicine with analgesic, antipyretic, and antimicrobial properties.

The inhibiting performances of Tantum rosa were evaluated by electrochemical techniques (potentiodynamic polarization and impedance measurements) and surface analysis (SEM-EDX). Several isotherms were tested for their relevance to describe the adsorption behavior of the tested drug. To the best of our knowledge, there have not been reported any other research addressing the corrosion inhibition performance of Tantum Rosa so far.

2. EXPERIMENTAL

2.1. Reagents and materials

The corrosive test electrolyte was a 3.5 wt.% NaCl aqueous solution (pH=5.5) prepared from analytical grade reagent (Merck, Darmstadt, Germany) and distilled water.

The drug tested as corrosion inhibitor was Tantum rosa (TR). The active component of Tantum rosa is benzydamine hydrochloride; its molecular structure is presented in Figure 1.

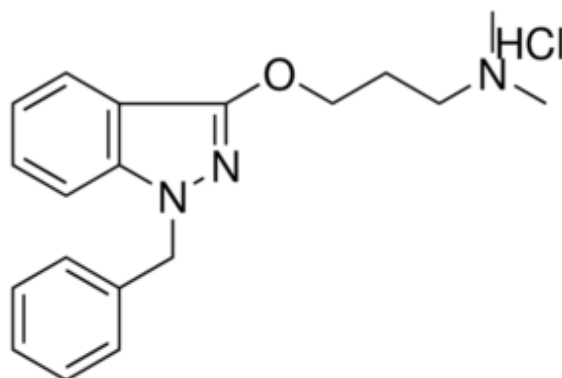


Figure 1. Molecular structure of benzydamine hydrochloride

The inhibitor-containing electrolytes were prepared by dissolving appropriate weighted amounts of TR drug in 3.5 wt.% NaCl solution, in order to obtain the following concentrations of inhibitor: 0.1, 0.5, 1, 5 and 10 mM, respectively.

2.2. Electrochemical measurements

The working electrode was a copper cylinder embedded in epoxy resin with an exposed area of 0.28 cm². The counter electrode was a platinum foil, while a saturated calomel electrode was used as reference.

Before the corrosion tests, the working electrode was mechanically abraded under a water stream with 2400 and 4000 grade silicon carbide papers, then polished with 0.3 μm alumina slurry to obtain a mirror-like surface. Finally, the copper electrode was rinsed thoroughly with distilled water, dried, and immediately immersed in the corrosive solution.

Electrochemical experiments were performed in a conventional three-electrode cell configuration, using a 2273 PAR potentiostat (Ametek, Berwyn, PA, USA). Before each experiment, the copper electrode was left at the open circuit potential (OCP) for 1 h in the test solution. Potentiodynamic polarization curves were recorded at a constant scan rate of 10 mV min⁻¹ over a potential range of ± 250 mV vs. OCP, from the cathodic to the anodic direction.

Electrochemical impedance spectra (EIS) were acquired at OCP in the frequency range 10 kHz to 10 mHz at 5 points per decade and with an AC voltage amplitude of ±10 mV. To evaluate the time-

stability of the inhibitor barrier film formed on the copper surface, EIS measurements were carried every hour in the first 10 h and then at 24 h and 48 h, respectively.

The impedance data were interpreted based on proper equivalent electrical circuits using the *ZSimpWin* 3.21 software (Ametek, Berwyn, PA, USA).

2.3. Surface characterization by SEM-EDX

The morphology of the copper surface was examined using a JSM 5600 LV scanning electron microscope (JEOL, Akishima, Tokyo, Japan), operated at 15 kV accelerating voltage. For this purpose, the copper samples were immersed in 3.5 wt.% NaCl solution in the absence and in the presence of TR. After 24 hours of exposure, the copper samples were taken out, gently washed with distilled water, and dried at room temperature.

The elemental analysis of the corrosion products formed on the metal surface was performed by an energy dispersive X-ray spectroscopy (EDX, Oxford Instruments, INCA 300).

3. RESULTS AND DISCUSSION

3.1. Potentiodynamic polarization curves

Potentiodynamic polarization experiments were carried out on copper samples immersed in 3.5 wt.% NaCl solution without and with the addition of various concentrations of TR. The obtained results are depicted in Figure 2.

From Figure 2, it could be seen that the addition of TR in the corrosive solution gives rise to a decrease of both anodic and cathodic current densities as compared to the blank solution. This behavior indicates that the tested drug is able to hinder to some extent the copper dissolution and the oxygen reduction processes.

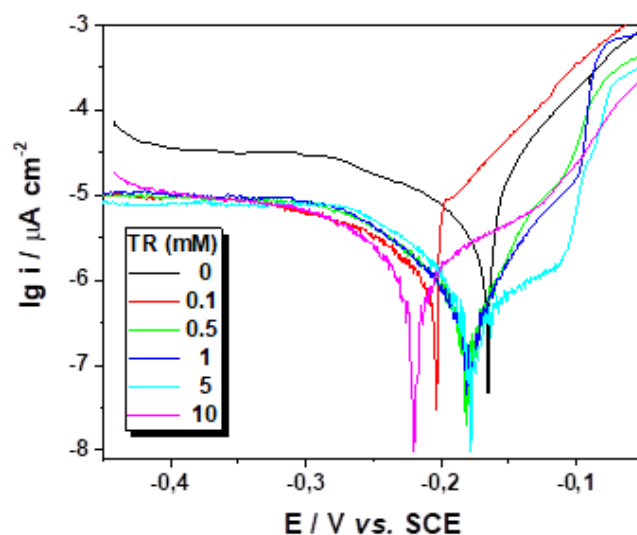


Figure 2. Potentiodynamic polarization curves of copper in 3.5 wt.% NaCl solution in the absence and in the presence of different concentrations of Tatum rosa drug

To yield a quantitative approach, the electrochemical kinetic parameters, such as the corrosion potential (E_{corr}), cathodic and anodic Tafel slopes (β_{c} and β_{a}) and corrosion current density (i_{corr}) were estimated using the Tafel extrapolation method. The obtained results are summarized in Table 1.

The inhibition efficiency values ($z\%$) calculated according to equation (1) are also presented in Table 1.

$$z(\%) = \frac{i_{\text{corr}}^0 - i_{\text{corr}}}{i_{\text{corr}}^0} \times 100 \quad (1)$$

where i_{corr}^0 and i_{corr} are the values of the corrosion current densities in absence and in presence of the inhibitor, respectively.

Table 1. Electrochemical parameters of copper in 3.5 wt.% NaCl solution, in the absence and in the presence of various concentrations of TR drug determined by Tafel extrapolation method

TR (mM)	E_{corr} (mV vs. ESC)	i_{corr} ($\mu\text{A cm}^{-2}$)	$ \beta_{\text{c}} $ (mV dec ⁻¹)	β_{a} (mV dec ⁻¹)	z (%)
0	-164	4.27	328	57	-
0.1	-203	2.17	218	40	49.2
0.5	-177	0.78	100	56	81.7
1	-179	0.51	73	43	88.1
5	-176	0.44	47	112	89.7
10	-217	1.33	210	123	68.9

The inspection of Table 1 reveals a progressive decrease of the corrosion current density values in the presence of increasing TR concentrations. The lowest i_{corr} value was obtained by addition of 5 mM TR; it was almost ten time smaller as compared to the corrosion current density value calculated for the blank solution. These results confirm the inhibiting effect of TR drug on the copper corrosion in 3.5 wt.% NaCl solution. In addition, a shift of the E_{corr} values towards more negative values could be noticed in the presence of all tested TR concentrations. Since the displacement of the E_{corr} values is less than ± 85 mV [34], it was assumed that the investigated drug behaves as a mixed-type inhibitor. Likewise, the changes of the Tafel slopes in the presence of TR indicate that the kinetics of both anodic and cathodic processes are affected by the inhibitor addition in the corrosive solution.

The inhibition efficiency values increase gradually with the inhibitor concentration from 49.2 % at 0.1 mM TR to the maximum value of 89.7% obtained in the presence of 5 mM TR. A further increase of the TR concentration to 10 mM leads to a decrease of its inhibiting efficiency.

A possible explanation for the inhibiting properties of TR could be found in its ability to adsorb on the metal surface developing a protective barrier film, which isolate the copper from the aggressive electrolyte, decreasing the corrosion rate. However, high concentration of TR in the solution could unfavorably influence the arrangement of the adsorbed molecules or the adsorption equilibrium reaction, which might explain the decline of its protective effect at 10 mM. A similar behavior was formerly noticed in the case of copper corrosion in the presence of 4-(pyridin-3-yl) thiazol-2-amine [35] and 1-octyl-3-methylimidazolium acetate [36].

3.2. Electrochemical impedance spectroscopy

In order to confirm the results obtained from the potentiodynamic polarization curves and to acquire more information on the influence of Tantom Rosa on the copper corrosion mechanism, concentration and time-dependent electrochemical impedance measurements were performed at the open-circuit potential.

Nyquist impedance diagrams obtained in solutions without and with the addition of TR drug at different concentrations are presented in Figure 3. Prior any impedance measurement, the copper electrode was left at the free corrosion potential for 1-h until a steady-state was attained.

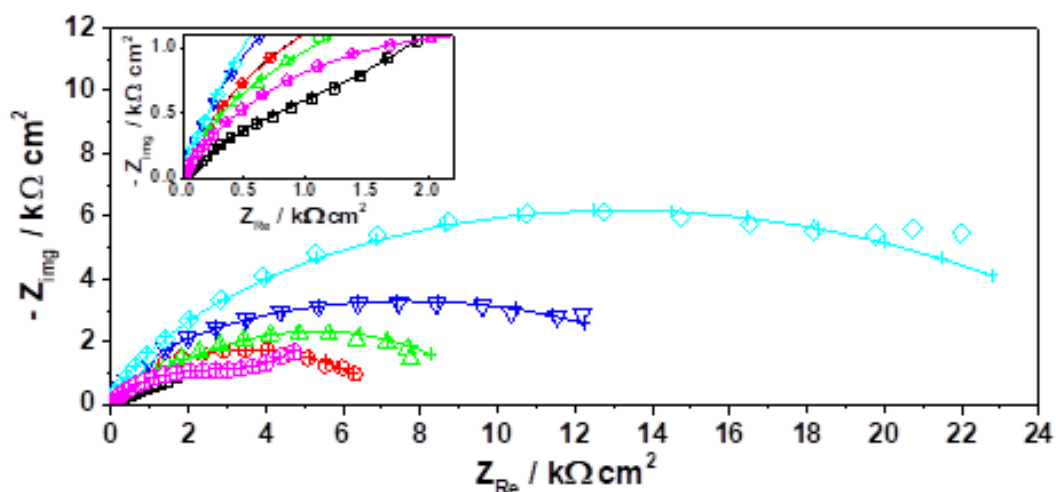


Figure 3. Nyquist diagrams recorded after 1-h immersion of copper in 3.5 wt.% NaCl solution in the absence and presence of different TR concentrations (mM): (\square) 0; (\circ) 0.1; (Δ) 0.5; (∇) 1; (\diamond) 5; (\diamond) 10. Symbols – experimental impedance data; (—+—) calculated impedance. *Insert:* Impedance diagrams in enlarged scale

As shown in Figure 3, the impedance spectra of copper recorded in the absence and in the presence of TR exhibit a capacitive behavior in the whole frequency range. The progressive enlargement of the impedance in the presence of increasing concentrations of TR up to 5 mM could be related to a gradual inhibition of the copper corrosion process. With further increase of TR concentration to 10 mM, a decrease of the impedance could be noticed in Figure 3, in agreement with the results of the polarization measurements, which also revealed the weakening of TR inhibiting properties.

Although not clearly seen in Figure 3, the impedance diagram recorded in the blank solution consists of two depressed capacitive loops at high and medium frequencies, and a straight line in the low frequency domain. A similar feature of the impedance spectra was noticed in the presence of 10 mM TR, while the diffusion tail vanishes at lower concentrations of inhibitor (≤ 5 mM).

The high frequency capacitive loop was ascribed to the corrosion product/inhibitor film formed on the copper surface in the absence and in the presence of TR drug. The capacitive loop at lower frequencies corresponds to the faradaic process of electrode reactions [37], while the Warburg tail could be attributed either to the diffusion of the soluble cuprous chloride complexes from metal surface to the bulk solution or to the transport of the dissolved oxygen towards the electrode [38]. The vanishing of the

Warburg impedance at certain concentrations of inhibitor (≤ 5 mM) confirms that TR drug is able to form a dense film on the copper surface that impedes the diffusion process.

Figure 4 shows the equivalent electrical circuits used for the fitting of the experimental EIS data obtained in the absence and in the presence of different TR concentrations.

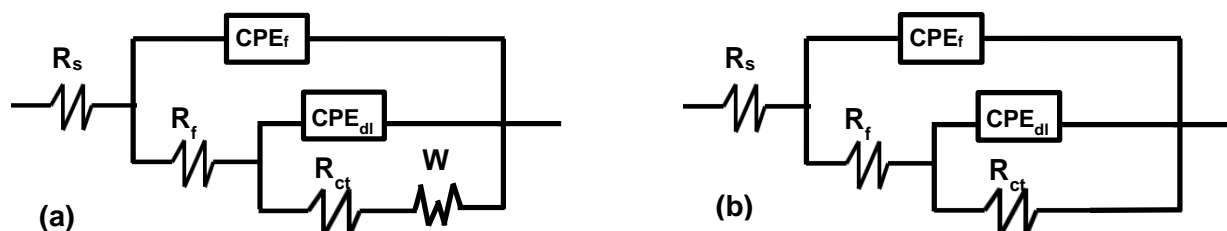


Figure 4. The electrical equivalent circuit models used to fit the EIS experimental data

Due to the depressed nature of the capacitive loops in Figure 3, constant phase elements (CPE) were used instead of pure capacitances to compensate for the surface roughness, inhibitor adsorption, porous layer formation and other surface inhomogeneities [39].

The impedance of CPE (Z_{CPE}) could be expressed as follows:

$$Z_{CPE} = [Y(j\omega)^n]^{-1} \tag{2}$$

where $\omega = 2\pi f$ is the angular frequency, $j = \sqrt{-1}$ is the imaginary unit, Y is the magnitude of the CPE and n is a fitting parameter ($0 \leq n \leq 1$) which evaluate the deviation from the pure capacitive behavior ($n = 1$) [40-42].

The Y parameters of the CPE elements were further converted in the associated capacitances (C), based on the equation [43]:

$$C = (R^{1-n} Y)^{1/n} \tag{3}$$

As previously reported [38], in the equivalent electric circuits from Figure 4, R_s is the solution resistance; R_f stands for the film resistance towards the access of the aggressive ions through the surface film modified by the inhibitor; CPE_f is the constant phase element modelling the film capacitance (C_f); R_{ct} represents the charge transfer resistance, while CPE_{dl} is associated to the double layer capacitance (C_{dl}) that appears at the electrode interface; W is the Warburg element.

The proper overlapping between the experimental impedance data and the calculated ones, observed in Figure 3, confirms the validity of the proposed equivalent circuits.

Table 2 summarizes the obtained values of the fitting parameters. The inhibition efficiency values, z , calculated from the charge transfer resistances, according to the equation (4) are also depicted in Table 2.

$$z (\%) = \frac{R_{ct} - R_{ct}^0}{R_{ct}} \cdot 100 \tag{4}$$

where R_{ct} and R_{ct}^0 are the charge transfer resistances in solutions with and without TR, respectively.

Table 2. Impedance parameters of copper in 3.5% NaCl solution without and with various concentrations of TR

Conc./ mM	$R_f /$ $k\Omega\text{ cm}^2$	$CPE_f /$ $\mu\text{F s}^{n-1}\text{ cm}^{-2}$	n_f	$C_f /$ $\mu\text{F cm}^{-2}$	$R_{ct} /$ $k\Omega\text{ cm}^2$	$CPE_{dl} /$ $\mu\text{F s}^{n-1}\text{ cm}^{-2}$	n_{dl}	$C_{dl} /$ $\mu\text{F cm}^{-2}$	$W /$ $\text{S s}^{1/2}\text{ cm}^{-2}$	$z /$ (%)
0	0.11	144.8	0.800	51.6	2.20	807.0	0.509	1400	0.0026	-
0.1	1.29	55.4	0.850	34.8	6.29	173.1	0.477	190	-	65.1
0.5	1.76	35.3	0.813	18.6	8.38	183.5	0.567	254.8	-	73.8
1	2.56	26.9	0.864	17.7	14.36	118.5	0.445	229.8	-	84.7
5	3.72	14.4	0.821	7.6	25.75	59.1	0.437	63.7	-	91.5
10	0.53	44.2	0.575	2.7	4.63	191.3	0.422	161.9	0.00199	52.6

According to Table 2, with the increase of TR concentration, the film resistance progressively rises from 0.11 $k\Omega\text{ cm}^2$ in the blank solution to the value of 3.72 $k\Omega\text{ cm}^2$ calculated in the presence of 5 mM TR. Jointly, the values of the film capacitances are much lower in the presence of TR. These results suggest that the film covering the copper surface in presence of TR is likely thicker, more compact, and protective than in its absence, which further makes the ionic conduction through this layer more difficult. However, the permeability of the surface film appears to be higher in the presence of 10 mM TR. Similar results were previously reported for other inhibitors at high concentrations [44, 37]. This behavior was explained by Huang and Guo [37] assuming that the interaction forces between the organic molecules might increase at high concentrations of inhibitor, which leads to the desorption of the inhibitor molecules or to the change of the adsorption morphology, which finally induce a decrease of the inhibition efficiency values.

The increased addition of TR in the corrosive solution leads to a gradual enhancement of the R_{ct} values up to 24.91 $k\Omega\text{ cm}^2$ at 5 mM TR, indicating that the charge transfer process becomes slower, likely due to the improved adsorption of the inhibitor on metal surface. As expected, at higher concentration of TR, the R_{ct} value decreases, although it remains lower as compared to the charge transfer resistance of the blank solution.

From Table 2, it could be also seen that the C_{dl} value for the blank solution is rather high, in agreement with the formation of coarse corrosion products on the copper surface during the dissolution process, which increases the active surface area. Nonetheless, an important decrease of the C_{dl} values occurs in presence of all tested concentrations of TR. This decay of the C_{dl} values may originate from the decrease of the local dielectric constant and/or the increase in the thickness of the electrical double layer, due to the gradual replacement of the water molecules by the adsorbed TR molecules, which form an adherent film on the copper surface, leading to a smaller electrode area directly in contact with the corrosive solution [28].

The highest inhibition efficiency values of 91.5% was obtained in the presence of 5 mM TR, which was therefore stated as the ‘optimum’ concentration in the investigated experimental conditions.

It is also worth mentioning that the z values estimated from the EIS interpretation are in reasonable agreement with those obtained from the potentiodynamic polarization measurements.

Figure 5 shows the influence of the immersion time on the impedance behavior of the copper exposed to 3.5 wt.% NaCl solution in the absence and in the presence of the optimum concentration of TR.

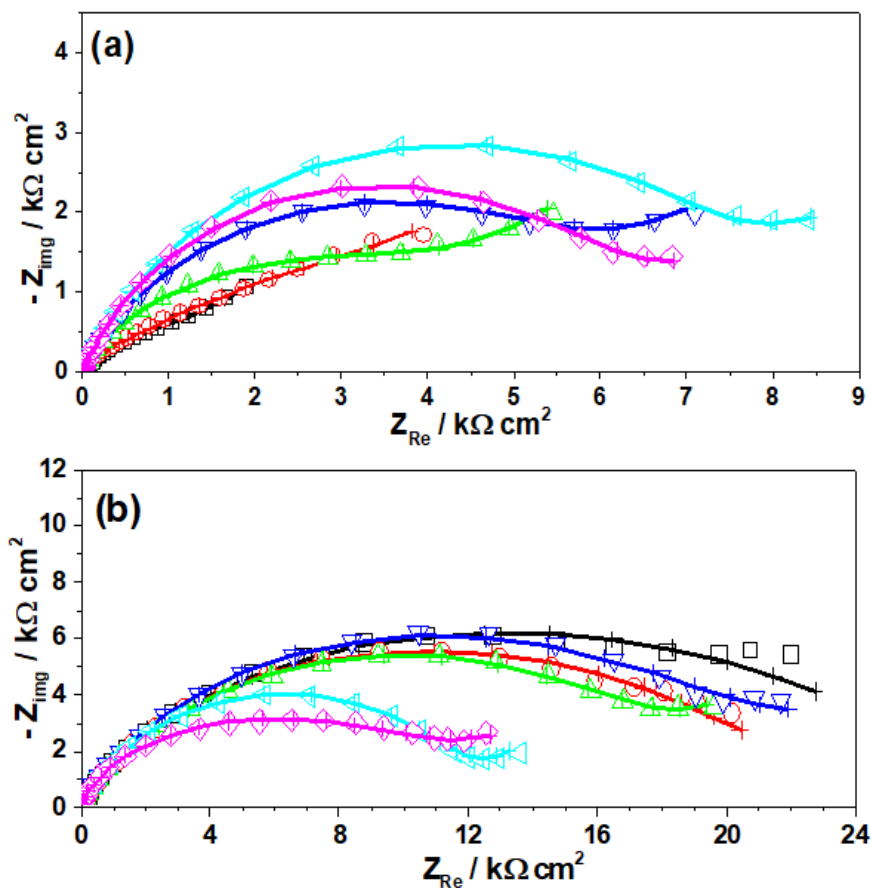


Figure 5. Nyquist diagrams for copper in 3.5 wt.% NaCl solution in the absence (a) and in the presence of 5 mM TR (b) at different immersion times (hours): (\square) 1; (\circ) 2; (Δ) 6; (∇) 10; (\triangleleft) 24 and (\diamond) 48. Symbols – experimental impedance data; (-+-) calculated impedance.

Comparing the EIS spectra obtained at different immersion times in the presence of 5 mM TR (Figure 5b), it could be seen that the impedance values decrease slightly within the first 10 h of exposure, while at longer exposure this descending trend become more evident. Besides, as the exposure time elapsed, a Warburg impedance appears in the low frequency region revealing the occurrence of a diffusional process.

The previously used equivalent circuits (Figure 4) were further employed to fit the experimental data from Figure 5. The time evolution of the calculated R-C parameters is illustrated in Figure 6.

As shown in Figure 6, TR is able to hinder the copper corrosion process during the entire exposure period, but its protective effect diminishes as the immersion time elapses. Thus, the R_f values obtained at in the presence of TR decreases in the first 6 h of immersion leading to a small enhancement of the corrosion process, as revealed by the modest decrease of the R_{ct} values. After that, both R_f and R_{ct} values present an increasing trend with the immersion time up to 10 h. At prolonged exposure the electrolyte starts penetrating through the inhibitor film reducing its resistance and leading to a reinforcement of the corrosion process. The variation of the C_f and C_{dl} values suggests that TR is able to quickly adsorb on the copper surface, but the stability of the protective barrier film is rather weak and

decreases over the time, most probably due to the desorption of TR molecules and/or to the diffusion process from the copper/electrolyte interface. Hippolyte et al. [30] have reported a comparable behavior in their work on copper corrosion in 3.5 wt.% NaCl solution in the presence of nicotinamide. These authors have justified the progressive decrease of the nicotinamide inhibition efficiency with the immersion time by the desorption of inhibitor molecule from the metallic surface.

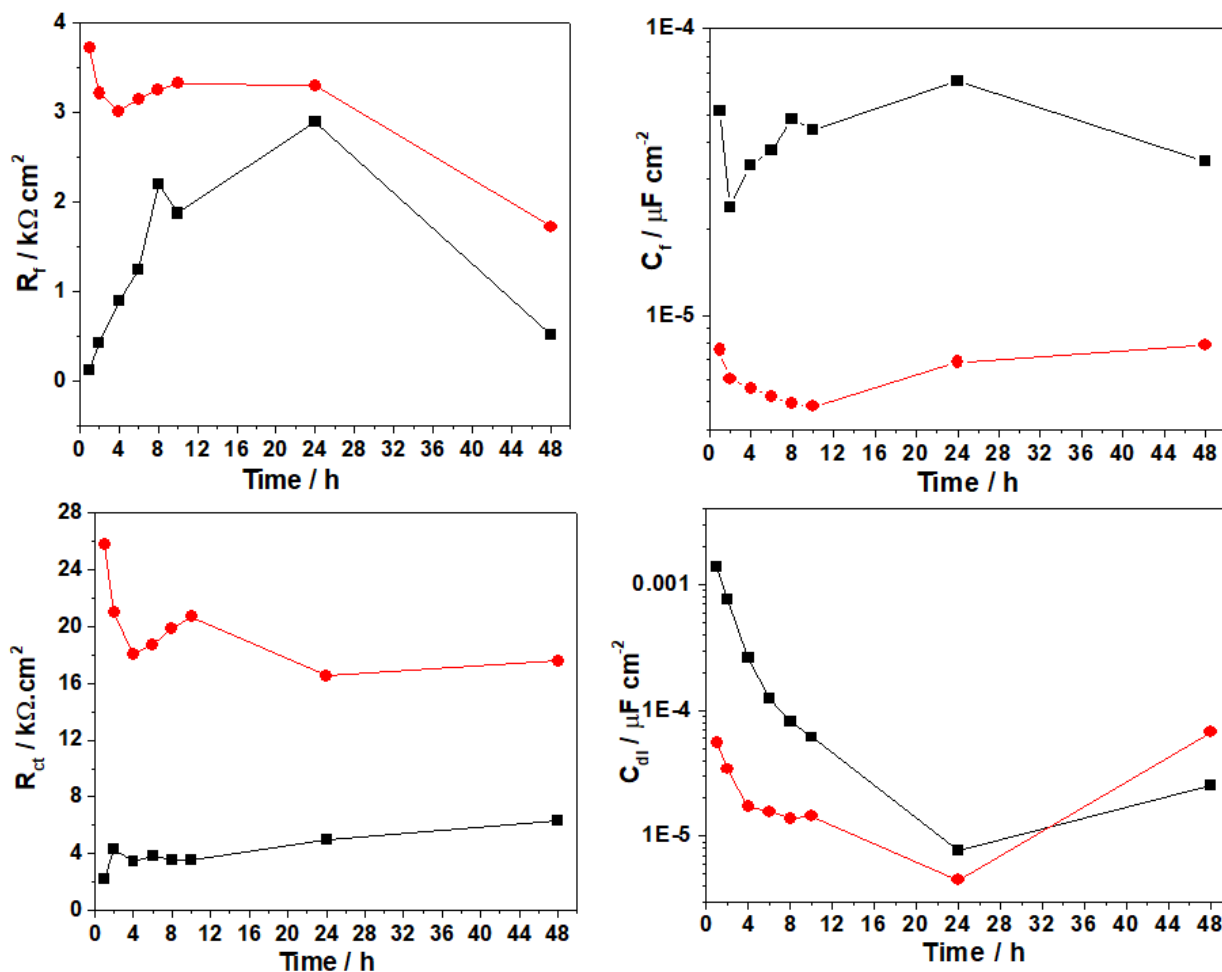


Figure 6. Influence of the immersion time on the calculated values of R-C parameters for copper corrosion in 3.5 wt.% NaCl solution in the (■) absence and in the presence of 5 mM TR (●)

The limited long-lasting protection afforded by TR on copper corrosion is also demonstrated by the inhibition efficiency values, which firstly decrease slightly with the immersion time from 1 h to 10 h (91.5% to 80%), but then after they fall to about 41% at 48 h of exposure.

3.3. SEM-EDX analysis

To further demonstrate the anticorrosive properties exerted by Tantum Rosa on the copper corrosion in 3.5 wt.% NaCl solution, SEM and EDX experiments were carried out.

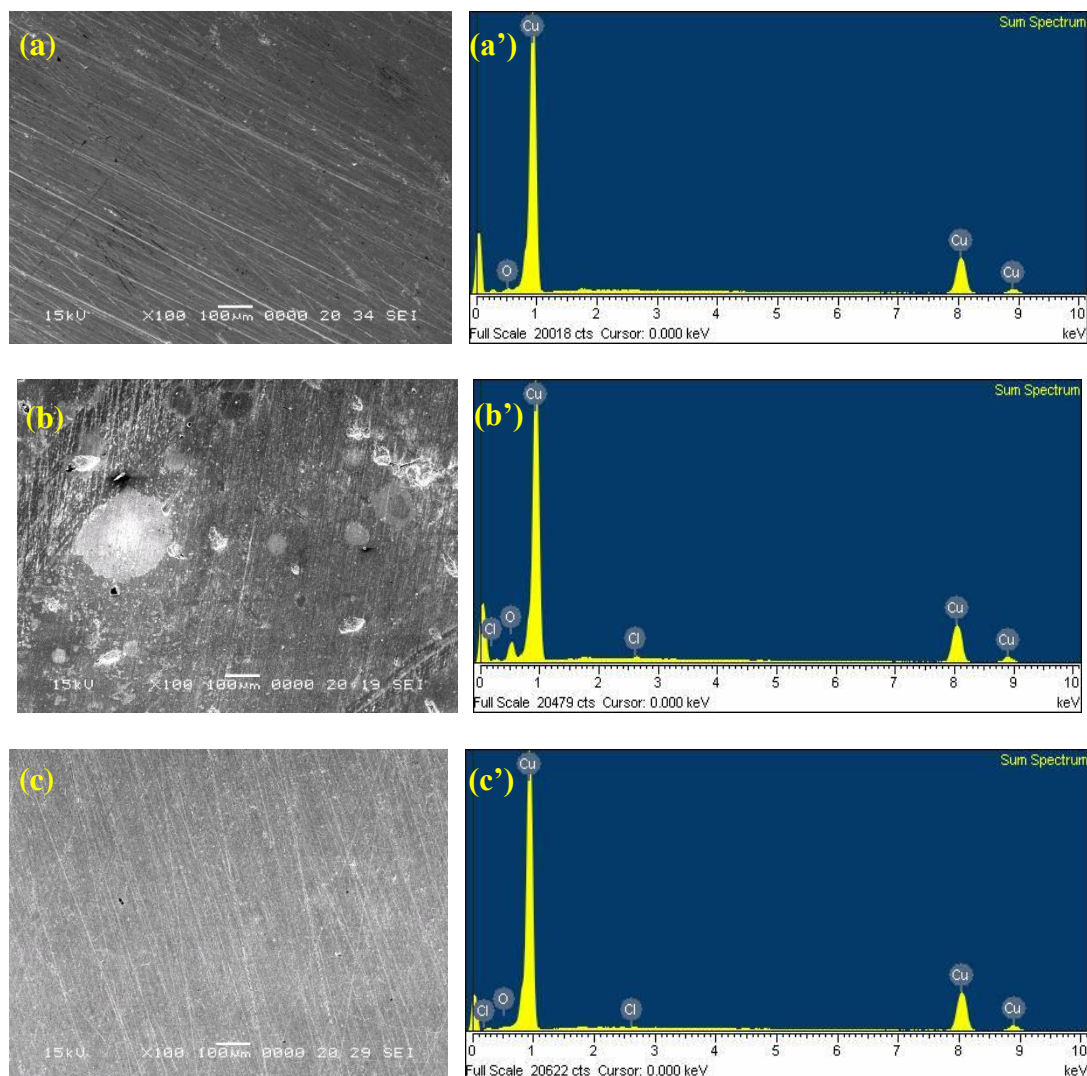


Figure 7. SEM micrographs (a, b, c) and EDX spectrum (a', b', c') of the newly polished copper sample (a, a') and of the copper specimen immersed for 24 h in 3.5 wt.% NaCl solution in the absence (b, b') and in the presence of 5 mM TR (c, c').

The SEM micrographs of the copper surface after 24 h immersion in saline environment, in the absence and in the presence of the optimum concentration of TR are illustrated in Figure 7, along with the corresponding EDX spectra.

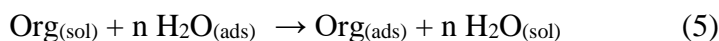
As shown in Figure 7a, before the immersion in the corrosive solution, the surface of the newly polished copper specimen was smooth, and the scratches caused by the grinding procedure are easily observed. Some small traces of copper oxides might be present on the metal surface, as proved by the low oxygen content identified in the EDX spectrum (Figure 7a').

After 24 h immersion in the 3.5 wt.% NaCl solution, the copper surface appears to be seriously damaged being covered with corrosion products, while some cracks and pits are also visible in Figure 7b. The increase of the atomic oxygen peak in the EDX spectrum from Figure 7b' correlates with the presence of the corrosion products, mainly consisting in copper oxides on the metal surface. However, the corrosive action of the saline solution on copper is diminished in presence of TR drug, as shown in Figure 7c, where a smooth surface with fine, visible scratches from the grinding procedure could be

observed. Likewise, the important decrease of the oxygen atomic peak in Figure 7c' confirms the ability of TR to impede the formation of corrosion products on copper surface.

3.4. Adsorption isotherm

It is well-known that the efficiency of the organic molecules to act as good corrosion inhibitors depends mainly on their adsorption ability on the metal. The adsorption process implies the replacement of the water molecules at a corroding interface, as follows [45]:



where $\text{Org}_{(\text{sol})}$ and $\text{Org}_{(\text{ads})}$ represents the organic molecules in the solution and adsorbed on the metal surface, respectively.

The use of the adsorption isotherms can provide important information on the nature of the interactions (physisorption and/or chemisorption) between the inhibitor molecule and the metal surface. For this purpose, the values of surface coverage degree, θ , were estimated from the EIS measurements, as a function of TR concentration, θ , assuming that its inhibiting efficiency is mainly due to the blocking effect of the adsorbed molecules on the copper surface and thus, $z = 100 \times \theta$ [46].

Several attempts were made to fit the surface coverage values into different adsorption isotherm models, such as Langmuir, Temkin, and Frumkin isotherms. The results showed that the Langmuir isotherm expressed by equation (6) provides the best description for the adsorption of TR on the copper surface [25]:

$$\frac{c_{\text{Inh}}}{\theta} = \frac{1}{K} + c_{\text{Inh}} \quad (6)$$

where c_{Inh} is the inhibitor concentration, and K represents the equilibrium adsorption constant.

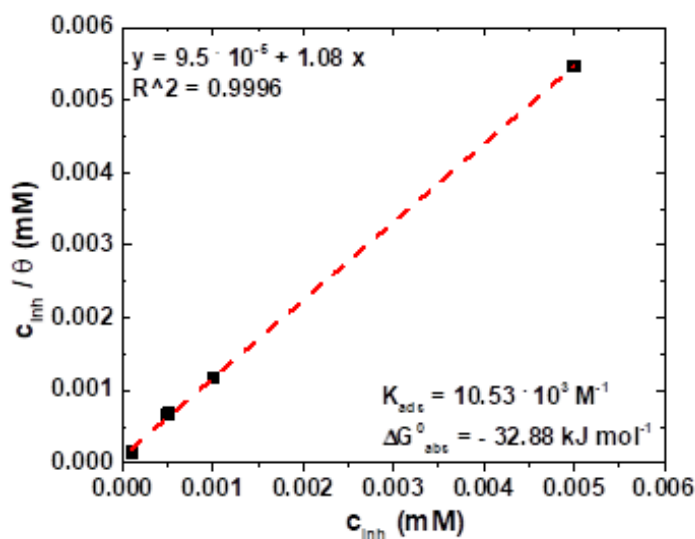


Figure 8. Langmuir adsorption isotherm of TR drug on the copper surface in 3.5 wt.% NaCl solution at 25°C.

The plot of $\frac{c_{Inh}}{\theta}$ versus c_{Inh} yields to a straight line with nearly unit slope and a correlation coefficient of 0.9996 (Figure 8) confirming that the adsorption of TR on the copper surface obeys the Langmuir isotherm.

Although the Langmuir isotherm approach describes an ideal monolayer adsorption of the inhibitor on homogeneous surface sites, with no lateral interaction between the adjacent adsorbed molecules [47] in real conditions, the functional groups usually grafted on the organic molecules could interplay through common repulsion or attraction forces. This explains the small deviation from unity of the slope of Langmuir plot (Figure 8).

The adsorption equilibrium constant (K_{ads}) was estimated from the intercept of Langmuir plot (Figure 8) and further used to estimate the standard free energy of adsorption (ΔG^0_{abs}), according to equation (7):

$$K = \frac{1}{55.5} \exp\left(\frac{-\Delta G^0_{ads}}{RT}\right) \quad (7)$$

where 55.5 represents the molar concentration of water in solution (mol dm^{-3}), R is the gas constant and T is the thermodynamic temperature.

Generally, when the values of ΔG^0_{abs} lay in the range from - 20 kJ mol⁻¹ to - 40 kJ mol⁻¹, the inhibitor adsorption is considered to be mixed adsorption, involving both physical and chemical interactions [48]. Values of ΔG^0_{abs} of - 20 kJ mol⁻¹ or less negative are associated to the electrostatic interactions between the inhibitor molecules and the metal surface (physisorption), whereas those of - 40 kJ mol⁻¹ or more negative reveal a chemisorption process [49].

In our study, the calculated value of ΔG^0_{abs} is - 32.88 kJ mol⁻¹. It suggests that TR drug acts through a combination of physical and chemical adsorption on the copper surface in 3.5 wt.% NaCl solution. The negative value of ΔG^0_{abs} also reveals the spontaneity of the adsorption process.

3.5. Comparative analysis with other commercial drugs

Table 3 displays a comparative analysis of the inhibiting performances of Tantum Rosa with those formerly reported for several commercial drugs used as corrosion inhibitors of copper in saline environments.

Table 3. Inhibiting performances for various studied commercial drugs on copper corrosion in saline environments

Studied commercial drug	Electrolyte	Concentration range	Inhibitor performances	Ref.
Azithromycin	0.9% NaCl	0.4 – 8 mM	$z^* = 76.67 - 95.14 \%$ Mixed-type inhibitor Adsorption follows Langmuir isotherm	[25]
Sulfathiazole	0.1 M NaCl	20 – 80 mg L ⁻¹	$z = 56.08 - 80.90 \%$ Cathodic-type inhibitor Adsorption obeys Langmuir isotherm	[26]
Domperidone	3.5 wt.% NaCl	5 – 25 mg L ⁻¹	$z = 80.06 - 93.6 \%$	[27]

			Anodic-type inhibitor Adsorption follows Langmuir isotherm	
Cephadrine	0.9% NaCl	0.1 – 5 mM	$z = 70 - 92.4 \%$ Mixed-type inhibitor	[28]
Doxepin	3.5 wt.% NaCl	0.1 – 10 mM	$z = 47.9 - 88.5 \%$ Mixed-type inhibitor	[29]
Nicotinamide	3.5 wt.% NaCl	1 – 11 mM	$z = 68 - 80 \%$ Mixed-type inhibitor Physical adsorption mechanism, according to Langmuir isotherm	[30]
Vitamin C	3% NaCl	1 – 3 g L ⁻¹	$z = 62.66 - 66.01 \%$ (weight loss)	[31]
Tantum Rosa	3.5 wt.% NaCl	0.1 – 5mM	$z = 49.2 - 89.7 \%$ Mixed-type inhibitor Physical and chemical adsorption mechanism, according to Langmuir isotherm	Present study

**Inhibition efficiency (z) values were determined from the potentiodynamic polarization measurements, except if other method is specified.*

The results obtained in the present paper suggest that the inhibiting properties of Tantum Rosa on copper corrosion are similar with those reported for other commercial drugs tested in saline environments. Thus, as discovered for Tantum Rosa in the present study, most of the previously tested drug molecules presented in Table 3 also inhibit the copper corrosion by adversely affecting the anodic and cathodic processes, thereby acting as mixed-type inhibitors, although in two cases cathodic or anodic predominance were also observed. They inhibit the corrosion by spontaneously adsorbing on the copper surface. In all cases, their adsorption mechanism obeys the Langmuir adsorption isotherm model. All drugs summarized in Table 3, including the novel proposed inhibitor (Tantum Rosa) show reasonably good inhibition efficiency at relatively low concentrations.

4. CONCLUSIONS

In the present work, the anticorrosive properties of the Tantum Rosa drug on copper in 3.5 wt.% NaCl solution were evaluated by electrochemical measurements and surface analysis. The following main conclusions could be drawn:

1. Tantum Rosa drug is able to inhibit to some extent the copper corrosion process, acting as a mixed-type inhibitor.
2. Polarization measurements show an enhancement of the inhibiting performances of Tantum Rosa with increasing its concentration up to 5 mM, when a maximum efficiency of 89.7% was achieved.
3. EIS measurements reveals that Tantum Rosa acts mainly through a spontaneous adsorption on the copper surface and formation of a thin protective film, which hinders the charge transfer process.

The time stability of the barrier film is rather weak leading to a decrease of the TR inhibition ability at prolonged exposure.

4. Adsorption of Tantum Rosa drug on copper is best described by Langmuir adsorption isotherm.

5. SEM-EDX analysis confirm the hindrance of the corrosion on copper surface due to the presence of Tantum Rosa.

ACKNOWLEDGMENTS

This research was carried out with the financial support of the "1 December 1918" University from Alba Iulia from the funds for scientific research. The authors kindly thank Dr. Florin Popa from the Materials Science and Engineering Department, Technical University of Cluj-Napoca (Romania) for SEM-EDX analysis.

References

1. E. M. Smale, T. C. G. Egberts, E. R. Heerdink, B. J. F. van den Bemt and C. L. Bekker, *Sustain. Chem. Pharm.*, 20 (2021) 100400.
2. C. Vatovec, J. Kolodinsky, P. Callas, C. Hart and K. Gallagher, *J. Environ. Manage.*, 258 (2021) 112106.
3. N. Vaszilcsin, D. Duca, A. Flueraş and M. Dan, *Stud U Babes-Bol Che*, LXIV (2019) 17.
4. S. Fekadu, E. Alemayehu, R. Dewil and B. Van der Bruggen, *Sci. Total Environ.*, 654 (2019) 324.
5. S.M. Zainab, M. Junaid, N. Xu and R.N. Malik, *Water Res.*, 187 (2020) 116455.
6. E. T. Furlong, A. L. Batt, S. T. Glassmeyer, M. C. Noriega, D. W. Kolpin, H. Mash and K. M. Schenck, *Sci. Total Environ.*, 579 (2017) 1629.
7. A. Toma and O. Crişan, *Clujul Med.*, 91 (2018) 391.
8. A. S. Fouda, S. M. Rashwan, M. Kamel and A. A. Badawy, *Int. J. Electrochem. Sci.*, 11 (2016) 9745.
9. F. E. Abeng, V. C. Anadebe, V. D. Idim and M. M. Edim, *S. Afr. J. Chem.*, 73 (2020) 125.
10. G. Gece, *Corros. Sci.*, 53 (2011) 3873.
11. C. Verma, D. S. Chauhan and M. A. Quraishi, *J. Mater. Environ. Sci.*, 8 (2017) 4040.
12. S. Tanwer and S. K. Shukla, *Current Research in Green and Sustainable Chemistry*, 5 (2022) 100227.
13. V. C. Anadebe, O. D. Onukwuli, F. E. Abeng, N. A. Okafor, J. O. Ezeugo and C. C. Okoye, *J. Taiwan Inst. Chem. Eng.*, 115 (2020) 251.
14. S. Sharma, R. Ganjoo, S. Kumar and A. Kumar, Evaluation of Drugs as Corrosion Inhibitors for Metals: A Brief Review. In: Ratan, J.K., Sahu, D., Pandhare, N.N., Bhavanam, A. (eds) *Advances in Chemical, Bio and Environmental Engineering CHEMBIOEN 2021*. Environmental Science and Engineering. Springer, Cham.
15. M. B. Petrović Mihajlović and M. M. Antonijević, *Int. J. Electrochem. Sci.*, 10 (2015) 1027.
16. C. Verma, *Science and Engineering of Green Corrosion Inhibitors: Modern Theory, Fundamentals & Practical Applications*, Elsevier, (2022) Amsterdam, Netherlands.
17. C. Verma, M.A.Quraishi and K. Y.Rhee, *J. Mol. Liq.*, 328 (2021) 115395.
18. L. T. Popoola, *Heliyon*, 5 (2019) e01143.
19. H. Lgaz, M. R.Al-Hadeethi, R. Salghic and H.-S.Lee, *Eco-Friendly Corrosion Inhibitors Principles, Designing and Applications*, Elsevier, (2022) Amsterdam, Netherlands.
20. S. Sharma and A. Kumar, *J. Mol. Liq.*, 322 (2021) 114862.
21. S. Karthikeyan, *Int. J. ChemTech Res.*, 9 (2016) 251.

22. E. Berdimurodov, A. Kholikov, K. Akbarov, L. Guo, S. Kaya, D. K. Verma, M. Rbaa and O. Dagdag, *J. Electroanal. Chem*, 907 (2022) 116055.
23. M. J. Baari and C.W. Sabandar, *Indones. J. Chem.*, 21(2021) 1316.
24. G. K. Shannamol, K. P. Sreelakshmi, G. Ajith and J. M. Jacob, *AIP Conf Proc* 2225 (2020) 070006.
25. Ž.Z. Tasić, M.B. Petrović Mihajlović, M.B. Radovanović and M.M. Antonijević, *J. Mol. Liq.*, 265 (2018) 687.
26. S. Zor, *Prot. Met. Phys. Chem. Surf.*, 50 (2014) 530.
27. D. Wang, B. Xiang, Y. Liang, S. Song and C. Liu, *Corros. Sci.*, 85 (2014) 77.
28. Ž.Z. Tasić, M.B. Petrović Mihajlović, M.B. Radovanović, A.T. Simonović, and M.M. Antonijević, *J. Mol. Struct.*, 1159 (2018) 46.
29. S. Varvara, R. Bostan, M. Popa, L. Gaina and F. Popa, *Stud U Babes-Bol Che*, LXV (2020) 215.
30. C. N. Hippolyte, B. Y. Serge, A. Sagne, J. Creus and T. Albert, *J. Mater. Sci. Chem. Eng.*, 6 (2018) 100.
31. M. V. Tomić, R. Fuchs Godec, Lj. Vasiljević and M. G. Pavlović, *Zaštita materijala*, 53 (2012) 201.
32. Ž. Z. Tasić, M. B. P. Mihajlović, M. B. Radovanović, A. T. Simonović and M. M. Antonijević, *J. Mol. Liq.*, 327 (2021) 114817.
33. I. Rotaru, S. Varvara, L. Gaina and L. M. Muresan, *Appl. Surf. Sci.*, 321 (2014) 188.
34. E. E. Oguzie, Y. Li and F. H. Wang, *Electrochim. Acta*, 53 (2007) 909.
35. R. Farahati, H. Behzadi, S. M. Mousavi-Khoshdel and A. Ghaffarinejad, *J. Mol. Struct.*, 1205 (2020) 127658.
36. H. Huang, B. Li, X. Zheng, J. Fan and M. Gong, *Int. J. Electrochem. Sci.*, 17 (2022) 220344.
37. H. Huang and X. Guo, *Colloids Surf. A*, 598 (2020) 124809.
38. W. Qafsaoui, M. W. Kendig, S. Joiret, H. Perrot and H. Takenouti, *Corros. Sci.*, 106 (2016) 96.
39. S. Varvara, C. Berghian-Grosan, R. Bostan, R. L. Ciceo, Z. Salarvand, M. Talebian, K. Raeissi, J. Izquierdo and R. M. Souto, *Electrochim. Acta*, 398 (2021) 139282.
40. J. R. Macdonald, *Impedance Spectroscopy*, John Wiley and Sons Inc., (1987) New York, USA.
41. J. B. Jorcin, M. E. Orazem, N. Pébère and B. Tribollet, *Electrochim. Acta*, 51 (2006) 1473.
42. C. H. Hsu and F. Mansfeld, *Corrosion*, 57 (2001) 747.
43. G. J. Brug, A. L. G. van den Eeden, M. Sluyters-Rehbach and J. H. Sluyters, *Electroanal. Chem.*, 176 (1984) 275.
44. R. Bostan, S. Varvara, L. Gaina and L. M. Muresan, *Corros. Sci.*, 63 (2012) 275.
45. R. Solmaz, *Corros. Sci.*, 52 (2010) 3321.
46. S. Varvara, R. Bostan, O. Bobis, L. Gaina, F. Popa, V. Mena and R. M. Souto, *Appl. Surf. Sci.*, 426 (2017) 1100.
47. C. M. Fernandes, L. X. Alvarez, N. Escarpini dos Santos, A. C. M. Barrios and E. A. Ponzio, *Corros. Sci.*, 149 (2019) 185.
48. Y. Liu, X. Yao, C. Liu, X. Luo, C. Guo and W. Du, *Int. J. Electrochem. Sci.*, 17 (2022) 220445.
49. H. Movahedinia, M. Shahidi-Zandi and M. Kazempour, *Int. J. Electrochem. Sci.*, 16 (2021) Article ID: 210228.